Solar Energy 174 (2018) 1185–1197

Contents lists available at ScienceDirect

Solar Energy

journal homepage: www.elsevier.com/locate/solener

A spatio-temporal city-scale assessment of residential photovoltaic power integration scenarios

G.B.M.A. Litjens*[,1], B.B. Kausika[1], E. Worrell, W.G.J.H.M. van Sark

Copernicus Institute of Sustainable Development, Utrecht University, PO Box 80.115, 3584CS Utrecht, the Netherlands

ARTICLE INFO

Keywords:
Self-consumption
Self-sufficiency
Battery storage
Electric vehicle

ABSTRACT

Cities have a significant potential to host residential photovoltaic systems (PV). The direct consumption of PV generated electricity reduces the need for electricity import, while excess PV electricity production can be stored for later usage or can be used directly to charge electric vehicles (EVs). In this way, more energy is locally consumed, greenhouse gas emissions are reduced, and self-sufficiency of cities can be increased. In this paper, we present a spatio-temporal framework to evaluate the electricity demand that can be fulfilled by PV energy. We assess the impact of penetration of EVs and the influence of battery energy storage. We demonstrate the usefulness of this framework for 88 neighbourhoods in the city of Utrecht, the Netherlands. Spatial mapping was used to identify areas with high potential for EVs and storage. Results shows that direct PV self-consumption ratios vary between 34% and 100%. When EVs charging is included in the neighbourhoods, then self-consumption is increased on average by 12%. Battery energy storage increases the self-consumption with an average of 25%. The self-sufficiencies due to direct PV energy consumption are between 6% and 40% in the neighbourhoods. These are decreased by EVs with an average of −0.6%, and increased by battery energy storage with an average of 14%. Avoided life cycle greenhouse gas emissions over a 30-year period are on average 12 tCO_2-eq per address. The large variation in results between neighbourhoods indicates that area dependent investments and supporting policies could improve the PV power integration in cities. Our developed framework can be easily adapted and used for other cities. Moreover, our results are useful for local governments to guide and design effective policies to accelerate the transition to more sustainable cities.

1. Introduction

Currently, cities host more than 50% of the global population and account for 70% of the global greenhouse gas (GHG) emissions (Acuto, 2016). One of the solutions to reduce CO_2 emissions from cities is the deployment of residential solar photovoltaic (PV) systems. Yet, PV system installation may be limited due to lack of suitable space. An added difficulty is the daily power fluctuation of the solar resources. This results in export of surplus PV electricity during daytime from cities and requires import of electricity during night time. Shifting energy demand to daytime results in higher PV self-consumption within cities and reduces CO_2 emissions from fossil-based backup power generation (Louwen et al., 2016).

The use of battery energy storage systems (BESSs) allows storage of surplus PV electricity to be used at later moments. The cost of BESSs is rapidly decreasing due to their increasing deployment (Schmidt et al., 2017). Currently, the number of electric vehicles (EVs) is rapidly increasing in the Netherlands, which increases the electricity demand within cities (Hoogvliet et al., 2017; van der Kam et al., 2018). BESS and EVs are becoming more economically attractive, especially due to cost reduction of Li-ion storage technology (Nykvist and Nilsson, 2015). Furthermore, EV costs are decreasing as a result of economic scaling effects. A shift from a gasoline-based car fleet to electric vehicles (EV) reduces emissions and air pollutants considerably, thereby contributing to improve air quality and quality of life in cities (Hawkins et al., 2012; Ajanovic and Haas, 2015).

Due to increased deployment of PV, EVs and domestic electric heating, it is expected that more overloading will occur on the medium voltage grid than on the low voltage grid, (Sijm et al., 2017). Consuming more PV generated electricity in the city can lower medium voltage distribution grid losses and reduces investments in cables and transformers. Smart EV charging and battery energy storage help to

* Corresponding author.
E-mail addresses: g.b.m.a.litjens@uu.nl (G.B.M.A. Litjens), b.b.kausika@uu.nl (B.B. Kausika), e.worrell@uu.nl (E. Worrell), w.g.j.h.m.vansark@uu.nl (W.G.J.H.M. van Sark).
[1] These two authors contributed equally.

https://doi.org/10.1016/j.solener.2018.09.055
Received 13 July 2018; Received in revised form 7 September 2018; Accepted 18 September 2018
Available online 26 October 2018

increase urban PV self-consumption (Mwasilu et al., 2014). For all these benefits, enhancement of PV self-consumption is seen as an important accelerator to reach a higher share of domestic PV installations and at the same time contribute to a reduction in greenhouse emissions (European Commission, 2015).

1.1. Literature review

Commonly, spatio-temporal PV potential in urban areas is assessed using geographic information systems (GIS) combined with numerical solar irradiation algorithms (Freitas et al., 2015; Kausika et al., 2015). PV integration studies focus mainly on using the generated PV electricity directly within the buildings or on community scale (Freitas et al., 2018; Luthander et al., 2015). Some studies combined the PV integration assessment with local or regional energy demand. Most of these studies assessed the provision of the net electricity consumption on an annual basis. A study assessed the potential of PV systems on rooftops and facades of 27 European countries. They found that the produced PV energy could provide in 22% of the projected 2030 annual electricity demand for these countries (Defaix et al., 2012).

A spatial model concluded that 2/3 of the current electricity demand could be covered by PV production for a small city in eastern Slovakia (Hofierka and Kaňuk, 2009). Of all the municipalities in Germany, 30% could be net self-sufficient when the full residential roof potential was used (Mainzer et al., 2014). In another study involving 34 German municipalities, it was found that 77% of the net electricity consumption could be provided by PV (Rodríguez et al., 2017). Furthermore, rooftop PV systems could provide 25% of the total annual electricity demand in Switzerland (Assouline et al., 2018). A study including a municipality in Sweden found that 88% of the annual demand can be provided with PV. Yet over 3000 h a year have more PV production than demand (Molin et al., 2016). A study of a city in Chile found that 24% of actual demand could be provided by PV, with the main limitation being the infrastructure of the grid (Wegertseder et al., 2016).

Few studies included temporal (hourly, daily) factors to assess the spatial potential of PV systems. A real-time platform containing a PV simulator and a distribution network simulator was presented and tested for the city of Turin, Italy. It was found that the actual distribution grid was not adequate to accommodate all PV generated electricity, if the available rooftop surface would be fully used (Bottaccioli et al., 2017). A PV penetration level of 40% was found for a German rural municipality to achieve a high PV self-consumption level (Camargo et al., 2015). Another spatio-temporal model analysed the impact of electric vehicles on the urban distribution network. This model provided insights in the critical local grid components that require upgrades for larger shares of electric vehicles (Mu et al., 2014). Only 27% of the electrical vehicles that are not in transit, are required to store excess PV produced power produced for the city of Yokohama, Japan (Yamagata and Seya, 2013).

1.2. Research aim

A limited number of studies are available that include both spatial and temporal effects of PV system integration. Furthermore, no research was found that assessed the spatial and temporal influence of electrical vehicles and storage on the PV self-consumption and PV self-sufficiency, except for a Dutch study with very coarse spatial resolution (van der Kam et al., 2018).

Therefore, this research aims to assess the role of EVs and BESSs for the PV self-consumption potential of a city. We developed a spatio-temporal framework that uses models to estimate the potential of PV yield, battery storage systems and electric vehicles. We demonstrate the framework using the city of Utrecht (the Netherlands) as a case study. The PV yield potential was assessed using the rooftop area of all residential buildings of this city. A time resolution of 5 min was used to assess the self-consumption and self-sufficiency potential at a neighbourhood level, over a 30-year lifetime. Neighbourhoods were identified that have surplus PV production to store in BESSs or charge EVs, or have limited PV yield production due to roof space limitations. Furthermore, we estimate the avoided life cycle GHG emissions due to PV electricity from two perspectives.

This study also includes socio-economic factors, e.g. household statistics and current number of cars in a neighbourhood. Two EV charging algorithms were incorporated, i.e., normal (uncontrolled) charging and smart solar charging. The latter charging method aims to charge EVs at moments with surplus PV power enhancing PV self-consumption. The results on each neighbourhood give information on the potential usageof the transformers within these neighbourhoods. The area of buildings connected to the transformers usually does not cross the borders of the neighbourhood. As a consequence, obtained results are valuable for distribution system operators (DSOs) to plan grid extensions and EV charging infrastructure. Furthermore, the results help local governments to design realistic and effective policies to develop carbon–neutral cities. The developed methodology can be modified and used for other cities and regions.

This study is arranged as follows. Section 2 explains the spatio-temporal framework and the used technical and environmental performance indicators. Section 3 presents the spatial results for the 88 neighbourhoods using maps of the city of Utrecht, the Netherlands. Section 4 assesses the sensitivity of the rooftop utilization rate, EV smart solar charging shares and battery storage capacities. Limitations concerning assumption, data availability and implementation challengers are discussed in Section 5 and the paper finalises with key conclusion in Section 6.

2. Methods

2.1. Spatio-temporal framework

A spatio-temporal framework was developed to combine spatial and temporal parameters. An algorithm was developed that combines time and location of PV production with time and location of electricity demand in the city. The main inputs of this algorithm are two time series for each neighbourhood: PV yield and total electricity consumption. The latter time series consists of the electricity consumption profile of buildings, with and without the consumption profile of electric vehicles. Both PV production and consumption time series are used in algorithms that determined self-consumption ratios and self-sufficiency ratiosover a lifetime of 30 years. An EV charging algorithm and BESS charging algorithm are used to assess the impact of EV and storage. An overview of the spatial level of the input data and model steps is shown in Fig. 1. We used reference parameters to compare the spatial self-consumption and self-sufficiency influence of the neighbourhoods, see Table 1. Also, the avoided life cycle GHG emissions from the PV systems are determined. The impact of the PV system potential on these parameters was assessed using four scenarios in the following sections:

- Neighbourhoods with PV systems only
- Neighbourhoods with PV systems and EVs
- Neighbourhoods with PV systems and BESS
- Neighbourhoods with PV systems, EVs and BESS

The framework was implemented using the city of Utrecht in the Netherlands. This city (latitude 52°05′38″ North, longitude 5°05′12″ East) is the fourth largest city in the Netherlands with 340,000 inhabitants. The city of Utrecht consists of 10 districts which make up 99 neighbourhoods. Neighbourhoods with 250 addresses or less were excluded from the analyses since these are mainly industrial or rural areas. As a result, 9 districts and 88 neighbourhoods were selected for the study. Each neighbourhood is made up of smaller areas that are

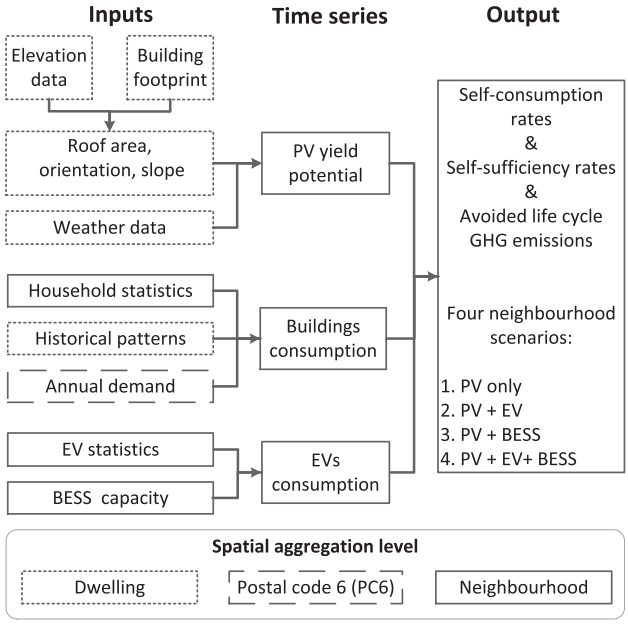

Fig. 1. Overview of the input data and model steps with corresponding spatial level to model the self-consumption ratios, self-sufficiency ratios and avoided life cycle greenhouse gas emissions for four scenarios.

Table 1
Main reference model input parameters.

Reference parameter	Value	Unit
PV capacity	200	Wp/m^2
Rooftop utilization factor	50	%
EV constant charging share	75	%
EV smart solar charging share	25	%
Relative battery storage size	1	$kWh_{BESS}\ MWh^{-1}_{demand}$
Relative battery inverter rating	0.5	$kW/\ kWh_{BESS}\ MWh^{-1}_{demand}$

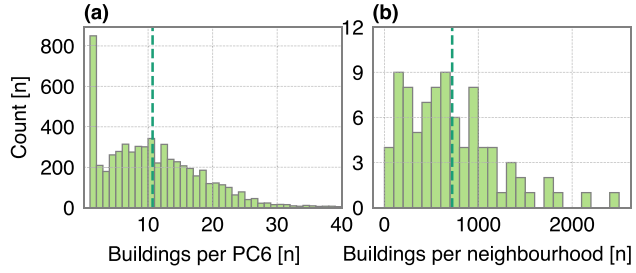

Fig. 2. Distribution of buildings containing residential addresses within each postal code 6 areas (a) and distribution of these buildings within each neighbourhood (b), both shown using a histogram. Mean values of the distribution are indicated by the dashed lines. Histogram bins of 1 building per postal code 6 and 100 buildings per neighbourhood were used. Note that 50 postal code 6 areas have more than 40 buildings and are not shown in histogram (a).

specified by a postal code 6 (PC6) level. A total of 63,494 buildings containing 132,671 residential addresses were used in the study. The distribution of buildings per PC6 area and within each neighbourhood is shown in Fig. 2. The majority of PC6 areas consist of a single building. The number of buildings within each neighbourhood shows a large variation.

2.2. PV yield potential

2.2.1. Roof statistics

The first step to assess the PV potential is the calculation of the roof statistics for each of the 63,494 buildings. The rooftop statistics consist of the roof area, orientation (azimuth and tilt) and the incoming plane of array (POA) irradiance. The incoming POA irradiance was determined using the Area Solar Radiation Tool of the ArcGIS Spatial Analyst (Environmental Systems Research Institute (Esri), 2017). The Area Solar Radiation tools calculated the POA irradiation across areas based on the hemispherical viewshed algorithm. These tools were developed by Rich et al. (1994) and further refined by Fu and Rich (2002).

The Area Solar Radiation tools calculations require a building footprint layer and a digital elevation model (DEM). The building footprint layer for the city of Utrecht was obtained from the Basisregistratie Adressen en Gebouwen (BAG) which was provided by the Dutch Cadastre, Land Registry and Mapping Agency (Het kadaster, 2016). The DEM was derived from high resolution elevation data, which was obtained from the Actueel Hoogte Bestand (AHN) Nederland (Actueel Hoogte Bestand Nederland, 2016). The DEM has a spatial resolution of 50 cm and was used as main input in the solar radiation tools. The roof area, slopes and azimuths for each roof top were calculated in GIS based on the DEM.

The default settings of the Area Solar Radiation Tool model were used containing the following default settings (Environmental Systems Research Institute (Esri), 2017). The latitudes for the buildings were calculated automatically based on the DEM metadata. Skysize was set to 200 and proved to be sufficient for time interval of 14 days. Horizon angles (number of calculation angles) are set to 32 which is adequate for complex topography. Diffusivity was set at 0.3 and transmissivity at 0.5 which is an indication of generally clear sky conditions. Using a fixed atmospheric value does impact the irradiation output on a smaller time scale (days or weeks). We observed that standard factors were sufficient to achieve a good fit with the measured values from the closest meteorological station (Royal Netherlands Meteorological Institute KNMI in De Bilt, The Netherlands).

The calculation took into account the effect of shadow due to nearby buildings, trees, and other roof obstacles like chimneys or gable style roofs. The digital surface model has been used as input for these calculations. The POA irradiation for each roof surfaces was calculated for the year 2015, with a 14 day interval. This time interval is used to calculate the sky sectors for the sun map (the sun's position in the sky across a period of time). These maps are used to calculate the total POA irradiance for a particular roof.

2.2.2. PV yield time series

The second step to determine the PV yield potential was to create a PV yield time series for each of the assessed rooftops. Buildings with addresses that have a residential function were selected from the building footprint layer. If a building contained only residential users than the full roof area was selected. However, some buildings have addresses with different functions, for example an office, shop or residence. For these buildings, the share of used surface for each function was obtained from the BAG dataset. The residential rooftop share was multiplied with the total roof area to define the roof area allocated for residential PV systems. We assumed that a maximum of 200 Wp/m^2 could be installed, based on a commercial available 320 Wp module with a dimension of 1.6 m by 1 m.

The PV yield timeseries was created using the open source Python package PVLIB (Andrews et al., 2014). The roof surface azimuth and tilt angles from the GIS model were binned to obtain 35 different combinations of roof slope and orientations. The roof surface azimuth angles were binned in steps of 45°, and roof slope angles in bins steps of 20°. A maximum tilt angle of 82.5° was selected. Facades were not included in our study. Furthermore, we assume that flat roofs will have a dual-tilt (or east–west) designed PV systems with a slope of 10°.

Radiation, wind speed, pressure and temperature data were obtained for 2015 from the Royal Netherlands Meteorological Institute KNMI in De Bilt, The Netherlands. The measurement intervals of radiation were 10 min and one hour for remaining weather parameters.

The weather data is linearly interpolated to 5 min interval and used as input for the PVLIB model. Furthermore, the module parameters of the Sanyo HIP-225HDE1 PV module are used to model the direct current (DC) PV yield time series (Panasonic, 2015). This module has a relative low temperature coefficient temperature thus reducing the influence of temperature in the model. The DC time series were converted to alternating current (AC) time series using the efficiency parameters of the Enphase Energy M210 inverter (Enphase Energy, 2015). The AC time series were linearly scaled to obtain a performance ratio of 85%, which is consistent with well performing PV systems in the Netherlands (Kausika et al., 2018).

Also, the PVLIB model calculate the total POA irradiance from the solar radiation data (no shading conditions). This number is used to determine the shade loss factor for each rooftop. This is the POA irradiance with shading (determined by the Area Solar Radiation tools) divided by the POA irradiance on a surface with no shading (determined using PVLIB). An average shade loss factor of 83% was found for all residential buildings. The shade loss factor was multiplied with the AC PV yield time series to determine the PV yield under shaded conditions.

Finally, the PV yield time series were scaled using a rooftop utilization rate. Only a certain part of the roof area can be used for PV modules due to constraints from other roof structures (chimneys, ventilation systems or dormers). We used a 50% roof utilization factor for PV systems, based on a previous study (Mainzer et al., 2014). The PV yield time series for each neighbourhood was created by aggregation of PV yield profiles for all buildings in that neighbourhood. The annual PV yield is reduced with 0.5% per year to account for PV system degradation (Jordan et al., 2016).

2.3. Electricity consumption from buildings

Electricity consumption time series were created for each neighbourhood using three main data sources; household statistics, historical residential demand time series and annual electricity consumption from residential grid connections. The household statistics from each neighbourhood in Utrecht are obtained from Statistics Netherlands (CBS) for 2015 (Centraal Bureau voor de Statistiek, 2016b). This data contains statistics on family compositions: people living alone, people living as a couple and couples with children.

Electricity demand profiles for 30 different households were measured between 2012 and 2014, by a Dutch distribution system operator (Liander N.V., 2016). The time series were measured using a 15 min time step for one year. Three new time series were created for each family composition using the 30 measured demand profiles. These three time series were scaled with share of family composition of each neighbourhood and summed together to create one demand time series per neighbourhood. The annual electricity consumption for each residential grid connection per postal code 6 area is available as open data for 2015 (Stedin Holding N.V., 2016). We assumed that each residential address has one grid connection. The electricity consumption of all residential addresses within a neighbourhood was summed to determine the annual electricity consumption of a neighbourhood. This number was used to linearly scale the neighbourhood demand time series. Finally, the neighbourhood demand time series were linearly interpolated to a 5-min time interval. The demand time series of one year were repeated to obtain a 30-year period. The average electricity consumption of households was quite stable for the last 10 years (Joost Gerdes and Sjoerd Marbus and Martijn Boelhouwer, 2016). Therefore, the annual demand is kept constant over the 30-year period.

2.4. Electric vehicle consumption

The number of registered cars per household in 2015 were obtained from CBS (Centraal Bureau voor de Statistiek, 2016b). The average number of cars within a neighbourhood was 932, with a minimum of 105 and a maximum of 2690. This corresponds to an average of 0.61 cars per household, with a minimum of 0.10 and a maximum of 1.05 cars per household. This is lower than the average for the Netherlands, which is 0.93 cars per household (Centraal Bureau voor de Statistiek, 2016a). Furthermore it is expected that electric vehicles will have a market share of 100% around 2040 (van der Kam et al., 2018). Therefore, we assumed that all current light duty gasoline vehicles will be replaced with electric vehicles. The daily power consumption of an EV depends on the average driving consumption multiplied by a seasonal factor. This factor accounts for the seasonal variability of the EV consumption mainly due to the cabin climate control and the battery efficiency. A seasonal factor of 0.8 was used for summer period and 1.2 for the winter period (Munkhammar et al., 2015). The summer period consists of the months June until August and the winter period December until February. Furthermore, we assumed an average driving power consumption of 7.24 kWh per day of which 50% will be charged within the neighbourhood (Centraal Bureau voor de Statistiek, 2016a). In addition, a EV charging and discharging efficiency of 90% was assumed (Hoogvliet et al., 2017). This results in a daily EV demand of 4.01 kWh and an annual demand of 1463 kWh.

The moments at which cars are connected to the charging stations are highly uncertain and are not well studied. Therefore we developed an algorithm to assess the impact of two different charging strategies on the EV integration potential. In the first strategy, the daily EV charging demand within a neighbourhood is gradually spread over the day. In this case, we assume that the summation of charging demands of each individual EV results in a flattened EV charging profile of a neighbourhood. Hence a constant EV consumption over the day was assumed. In the second option, the EV is directly charged with the produced PV energy. We call this option smart solar charging (van der Kam and van Sark, 2015). In this case, the EV is charged with the excess PV production in the neighbourhood. A maximum charging capacity of 11 kW per EV was assumed, to reduce the impact on the electricity grid. If adequate PV production is not available during the day, then the remaining charging demand is fulfilled when the solar elevation angle is < 0. Thus the EV demand is charged using the electricity grid. The charging profiles of both strategies were added to the neighbourhood electricity consumption profile. In the reference case, we assume that 75% of cars are charged using the first strategy and 25% of cars using the second strategy.

The distribution of residential neighbourhood annual electricity consumption including EV charging and the EV share are shown in Fig. 3. The total annual electricity consumption per neighbourhood ranges between 1 GWh and 16.3 GWh, with an average of 6.7 GWh. The share of EV consumption varies between 1.8% and 30.1%, with an average of 20.6%. These numbers show that there is a larger diversity of electricity consumption within each neighbourhood, mainly related to the number of inhabitants. Also, the EV charging demand within the neighbourhood is assumed to be constant over the 30-year assessment period. The total electricity demand of the 88 neighbourhoods is 466

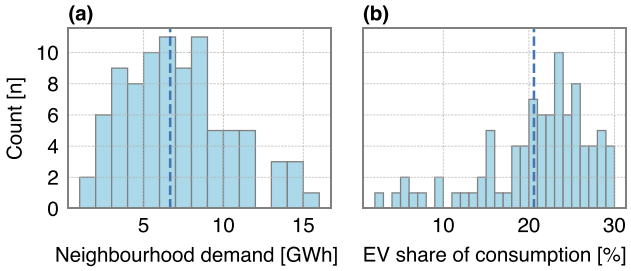

Fig. 3. Distribution of residential neighbourhood annual electricity consumption with EVs (a) and share of electricity consumption by EV charging (b) shown using a histogram. Mean values of the distribution are indicated by the dashed lines. Histogram bins of 2.5 GWh for neighbourhood energy demand and 1% for EV share were used.

GWh excluding EV charging and 587 GWh including EV charging.

2.5. BESS charging algorithm

Battery charging and discharging was simulated with a simple control strategy, obtained from previous research and written in Python (v3.5) (Litjens et al., 2018a). If more PV electricity is generated than consumed by the neighbourhood, then the battery was charged. If more electricity was consumed than generated, then the battery was discharged. The battery was discharged to fulfil electricity demand of the building. If the battery inverter and battery storage capacity was available, then the battery was also used to charge the electric vehicle.

An AC-coupled PV-battery system was assumed. This means that the PV array is connected via an inverter to the electricity grid and the battery storage pack with a battery inverter to the electricity grid. This is a commonly installed system type and is very suitable for retrofitting or installing community energy storage systems (Hoppmann et al., 2014). A battery storage capacity of 1 kWh battery storage capacity per MWh of annual electricity consumption per neighbourhood is used in the reference case (Hoppmann et al., 2014). Note that if EVs were included in the modelling, than the annual consumption in neighbourhoods is higher and thus larger battery sizes are used.

The battery inverter capacity is set to a C-rate of 0.5, meaning that it would require 2 h to fully charge the battery. Battery state of charge (SOC) is set to a minimum of 0% and a maximum of 100%. In this way, we assess the maximum storage potential to enhance self-consumption. Battery inverter efficiencies were obtained from the inverter efficiency curve of a SMA Sunny Boy Storage inverter, using a step size of 0.01% (SMA Solar Technology AG, 2017). A constant battery roundtrip efficiency of 92% was used, close to the round trip efficiency of a Tesla Powerwall (Tesla Motors, Inc., 2016). Furthermore, a calendric lifetime of 15 years and a battery cycle lifetime of 5000 full equivalent cycles is used to model the battery capacity degradation (Truong et al., 2016). The amount of diminished storage capacity is determined annually and subtracted from the previous year. The battery degradation model is explained in detail in a previous study (Litjens et al., 2018b). We assume that the battery storage is replaced after 15 years, thus the storage capacity is set similar to the original storage capacity for year 16.

2.6. Calculation of PV integration indicators

Two temporal PV integration indicators were assessed: self-consumption ratio (SCR) and self-sufficiency ratio (SSR). Self-consumption ratio is used to quantify the share of electricity that is self-consumed from the total annual produced PV energy. Self-sufficiency ratio is the share of electricity consumption that is fulfilled by PV electricity.

The self-consumed power consists of the total direct consumed power by the neighbourhood ($P_{\text{direct-consumed}}$) and the total power that is used for charging the battery ($P_{\text{B charge}}$). The direct consumed power is the PV power (P_{PV}) that is directly consumed as a result of the electricity demand of a building. (P_{demand}). The self-consumed energy is aggregated over the year from timestep (t = 1) till the last time step (t_{end}), see Eq. (1).

$$P_{\text{direct-consumed}} = \begin{cases} P_{\text{PV}} & \text{if } P_{\text{PV}} < P_{\text{demand}} \\ P_{\text{demand}} & \text{if } P_{\text{PV}} \geqslant P_{\text{demand}} \end{cases} \quad (1a)$$

$$\text{SCR} = \frac{\sum_{t=1}^{t_{\text{end}}} (P_{\text{direct-consumed,t}} + P_{\text{B charge,t}}) \cdot \Delta t}{\sum_{t=1}^{t_{\text{end}}} P_{\text{PV,t}} \cdot \Delta t} \quad (1b)$$

Self-sufficiency ratio is an indicator for the share of electricity consumption that is fulfilled by using PV electricity. This is the share of electricity demand that is fulfilled by the direct consumed PV power and the discharged power that is discharged from the battery ($P_{\text{B discharge}}$), see Eq. (2).

$$\text{SSR} = \frac{\sum_{t=1}^{t_{\text{end}}} (P_{\text{direct-consumed,t}} + P_{\text{B discharge,t}}) \cdot \Delta t}{\sum_{t=1}^{t_{\text{end}}} P_{\text{demand,t}} \cdot \Delta t} \quad (2)$$

2.7. Calculation of avoided life cycle GHG emissions

A rough indication of the avoided life cycle GHG emissions by the PV systems and battery energy storage systems was provided. Emissions due to manufacturing of the PV systems and BESS (GHG_{mfg}), and the avoided emissions by the PV electricity production are determined. The emissions of manufacturing the PV system depends on the production location (Louwen et al., 2016). We assume that PV systems are made in China as this country produces the majority of the PV cells and PV modules globally (Masson et al., 2017). Emissions from producing PV systems in this country are assumed to be 1590 gCO_2-eq for each Wp (de Wild-Scholten, 2013). The production of Li-Ion battery energy storage systems uses 110 gCO_2-eq for each Wh (Peters et al., 2017). We assumed that emissions from manufacturing a battery inverter are comparable to the emissions from manufacturing a PV inverter and assumed 124 gCO_2-eq per W. de Wild-Scholten (2013). The PV and battery inverter, and the battery storage are replaced after 15 years. Emissions from manufacturing are expected to be 25% lower when these components are replaced.

The avoided emissions by PV electricity production depend on the emission factor of electricity (EFE) from the grid. We assume that these emissions will reduce linearly from current emissions (2016) to zero emissions in 2050, based on the Dutch energy agreement for sustainable growth (Sociaal-Economische Raad, 2015). Thus, the carbon intensity will decrease linearly from 490 gCO_2-eq per kWh in year 1 to 60 gCO_2-eq per kWh in year 30 (Centraal Bureau voor de Statistiek, 2018).

The avoided emissions are determined for two system perspectives, i.e., from an electricity system perspective ($\text{GHG}_{\text{system}}$) and from a neighbourhood perspective ($\text{GHG}_{\text{neighb}}$). In the electricity system perspective, all PV electricity that was used is allocated as replacing electricity from the grid. The PV power that was used from a system perspective ($P_{\text{PV system}}$), is the PV produced power minus the battery energy storage losses. In the neighbourhood perspective, all PV power used within the neighbourhood is allocated as replacing electricity from the grid. Hence, avoided emissions from electricity exported to the grid are not included in this perspective. The PV power used ($P_{\text{PV neighb.}}$), is the sum of the direct consumed PV and the electricity discharged from storage. The used PV electricity of both perspectives was multiplied with the carbon intensity of the electricity grid for each year. Then, the emissions from manufacturing were subtracted from the total emissions over 30 years to determine the avoided life cycle GHG emissions. The avoided emissions are normalized with the number of addresses within a neighbourhood ($\text{N}_{\text{address}}$), see Eq. (3).

$$P_{\text{PV system}} = P_{\text{PV,t}} - P_{\text{B charge}} - P_{\text{B discharge}} \quad (3a)$$

$$P_{\text{PV neighb.}} = P_{\text{direct-consumed}} + P_{\text{B discharge,t}} \quad (3b)$$

$$\text{GHG}_{\text{system}} = \frac{\sum_{t=1}^{t_{\text{end}}} (EFE,\ t \cdot P_{\text{PV system,t}}) - \text{GHG}_{\text{mfg}}}{\text{N}_{\text{address}}} \quad (3c)$$

$$\text{GHG}_{\text{neighb.}} = \frac{\sum_{t=1}^{t_{\text{end}}} (EFE,\ t \cdot P_{\text{PV neighb.,t}}) - \text{GHG}_{\text{mfg}}}{\text{N}_{\text{address}}} \quad (3d)$$

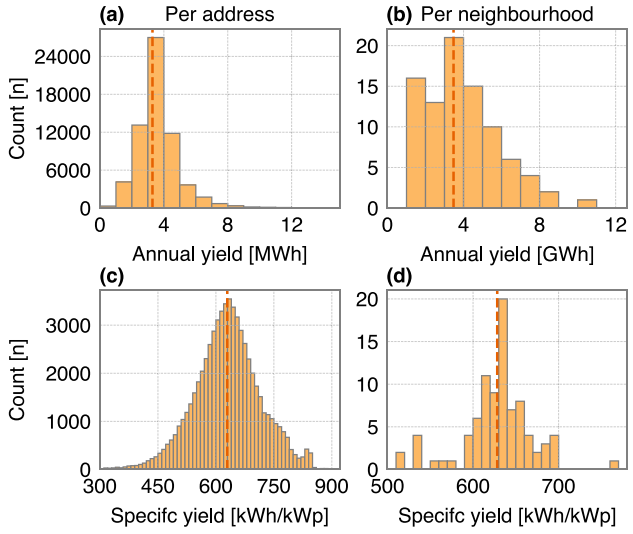

Fig. 4. Distribution of average annual PV yield for each address (a), average annual PV yield for each neighbourhood (b), average annual specific yield for each address (c) and average annual specific yield for each neighbourhood (d). Mean values of the distributions are indicated by the dashed lines. Annual yield is shown using bins of 1 MWh for each address and 1 GWh of each neighbourhood. Specific yield is shown using bins of 10 kWh/kWp. Note that 198 addresses have an annual yield higher than 15 MWh and are not shown on the histogram (a). Also 138 addresses with a specific yield of lower than 300 kWh/kWp are not shown on the histogram (c).

3. Results

3.1. PV yield potential

The PV yield potential for each of the 88 neighbourhoods was analysed over a period of 30 years using the reference parameters given in Table 1. The distributions of average annual PV yield for each address and the average annual PV yield for each neighbourhood are shown in Fig. 4. Also, the average annual specific yield for each address and each neighbourhood is presented. Average annual PV yield is 3.3 MWh per address and for the neighbourhoods 3.5 GWh. The specific yields show a larger distribution range for the addresses, with an average of 629 kWh per kWp. Specific yield for neighbourhoods is between 513 and 773 kWh/kWp, with an annual average of 628 kWh per kWp. The average specific yield decrease from 677 kWh/kWp in the first year to 579 kWh/kWp in year 30 due to PV system degradation. This specific yield is significantly lower than the current average specific yield for the Netherlands (Kausika et al., 2018). This is mainly due to the inclusion of all orientations and the reduced incoming irradiance due to shading. The total PV capacity from all neighbourhoods is 488 MWp and the average annual production 306 GWh.

The ratio between the total PV production and the total electricity consumption for a period of 30 years provided an indication on the contribution of PV to fulfil the electricity demand. This ratio is shown for each of the 88 neighbourhoods of the city of Utrecht in Fig. 5. The ratio is shown for two scenarios, only PV systems and PV systems with EVs. A ratio higher than 100% shows that there is more PV production than electricity consumption. This is the case for 5 neighbourhoods in the PV only scenarios. Neighbourhoods with PV systems only show an average of 68% and neighbourhoods with PV systems and EVs 53%.

3.2. Impact of PV systems only

The spatial impact of PV systems on the self-consumption ratio and self-sufficiency ratio for each neighbourhood is visualized using on a color-coded map in Fig. 6. Results are shown for 88 neighbourhoods which are separated by grey borders. The 9 districts are separated with

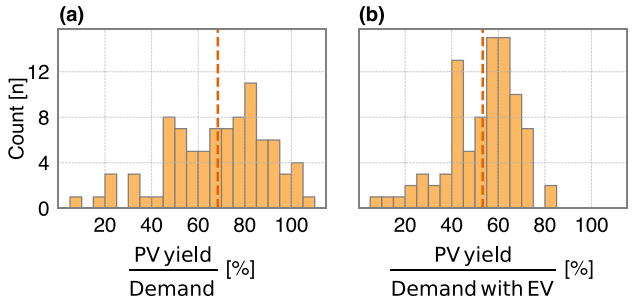

Fig. 5. Distribution of ratio between the total PV production and the total consumption of neighbourhoods with PV systems only (a) and neighbourhoods with PV and EVs (b) Mean values of the distribution are indicated by the dashed lines, and bins of 5% were used.

solid black lines and the district names are indicated. The white areas are those neighbourhoods of the city of Utrecht that were excluded from the study. For example, the left most neighbourhood in district West is actually a commercial area with a limited amount of residential dwellings.

The average SCR of the neighbourhoods is 53%, which demonstrates that the PV produced in a neighbourhood can be used most within the same neighbourhood. Moreover, a wide range of SCR between 34 % and 100% demonstrates a large variety in PV integration potential. Low SCR is seen for the suburb of Leidsche Rijn, and in the Noordwest (North-West) district, indicating a large surplus of produced PV energy. These areas contain mainly terraced houses with sufficient roof space available for PV systems.

High SCR was observed in the historical Binnenstad (Inner-city), Oost (East) and Overvecht districts. The inner-city area has a limited PV potential due to high concentration of historical buildings with relatively small roof areas and a high variation in roof shape and height. These roofs induce shading which reduces the plane-of-array irradiance and as a consequence the PV electricity generation. In addition, population density in the inner city is larger compared to other districts due to the smaller dwellings and apartments. This results in relatively high electricity consumption per unit area and thus a higher SCR. The district of Overvecht contains tall (mostly 10-storey) residential apartment buildings that limit the PV production potential per resident. Also, the district to the extreme East, in which the university campus is located, shows a high SCR. In this area, tall apartment buildings, which serve as student housing are located. Therefore, the roof area available per address is small.

An average SSR of 33% was determined for the neighbourhoods, ranging from 6% to 40%. Low SSRs are observed for the inner-city area, indicating that PV potential is not sufficient to fulfil the electricity demand. Higher self-sufficiency is observed for the suburb Leidsche Rijn, and in the Zuid (South) district. Areas with high SCR and low SSR have limited area to install PV systems and therefore limited PV yield. Areas with relatively lower SCR and higher SSR have more moments in which surplus of PV energy production occurs. The limited SSR indicates that the PV yield potential is not sufficient and electricity import to the city is a requirement.

3.3. Impact of EVs or BESSs

The influence of two scenarios, PV systems with EVs and PV systems with BESSs, on the self-consumption enhancement is presented in Fig. 7. Deployment of BESSs shows a larger impact on the SCR than the deployment of EVs. The replacement of gasoline-based cars by EVs results in an average increase in SCR of 12% points in the neighbourhoods. The SCR increase varies between 0% and 17% points, showing a broad impact of electric vehicles. Neighbourhoods with already high self-consumption due to the electricity consumption of the residential buildings show limited SCR enhancement by electric vehicles. The

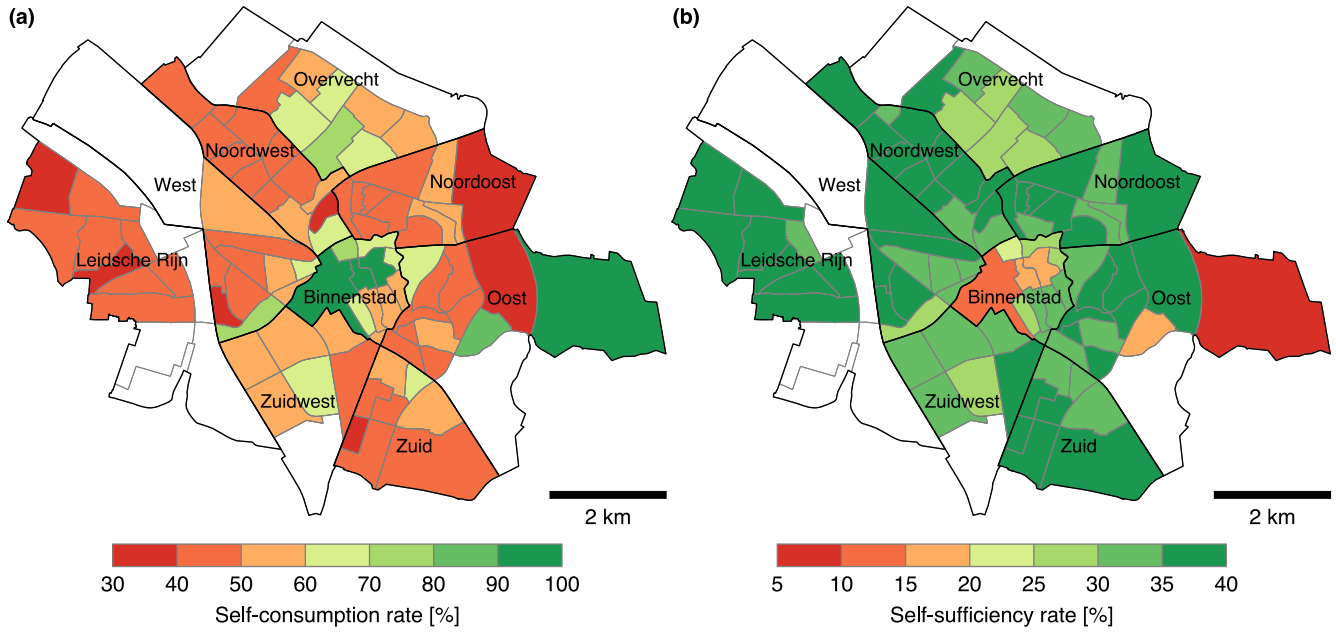

Fig. 6. Potential PV self-consumption ratio (a) and self-sufficiency ratio (b) for 88 neighbourhoods with only PV systems, for the city of Utrecht.

average self-sufficiency of neighbourhoods with introduction of EVs has barely changed. Observed differences in SSR are between −2.0% and 0.1% points with an average of −0.7% points. Only for two neighbourhoods EVs have a positive impact on SSR, namely Rijnsweerd and Hoge Weide. These neighbourhoods are in the Oost (East) and the Leidsche Rijn districts, respectively. The Rijnsweerd neighbourhood also has the lowest SCR without EVs. This shows that for almost all neighbourhoods the additional EV demand increases the need for imported electricity.

An average SCR increase of 25% points can be achieved with a battery capacity of 1 kWh for each MWh of electricity consumption. The SCR enhancement varies between 0% and 30% points. Neighbourhoods with a low self-consumption of PV systems only (Leidsche Rijn) have a SCR impact of ≈20% points from battery storage. In this case, the influence is limited by the battery storage capacity. The neighbourhoods with a high initial SCR (Binnenstad) have a limited BESS impact since most of the electricity is directly consumed anyway and the storage capacity is not utilized. Neighbourhoods with an initial self-consumption of around 60% (Overvecht) show the largest self-consumption impact. These neighbourhoods can store most surplus PV production and utilize the storage capacity. In addition, the SSR impact by storage varies between 0% and 18% points with an average of 14% points. As a result, 42 neighbourhoods obtain a self-sufficiency ratio > 50%

For a dwelling owner with a PV system, it could be advantageous to use storage under certain economic conditions (Schram et al., 2018). However, if this dwelling is located within a neighbourhood with low impact of storage on self-consumption, then this electricity could better be used by dwellings with insufficient roof space for a PV system. As a

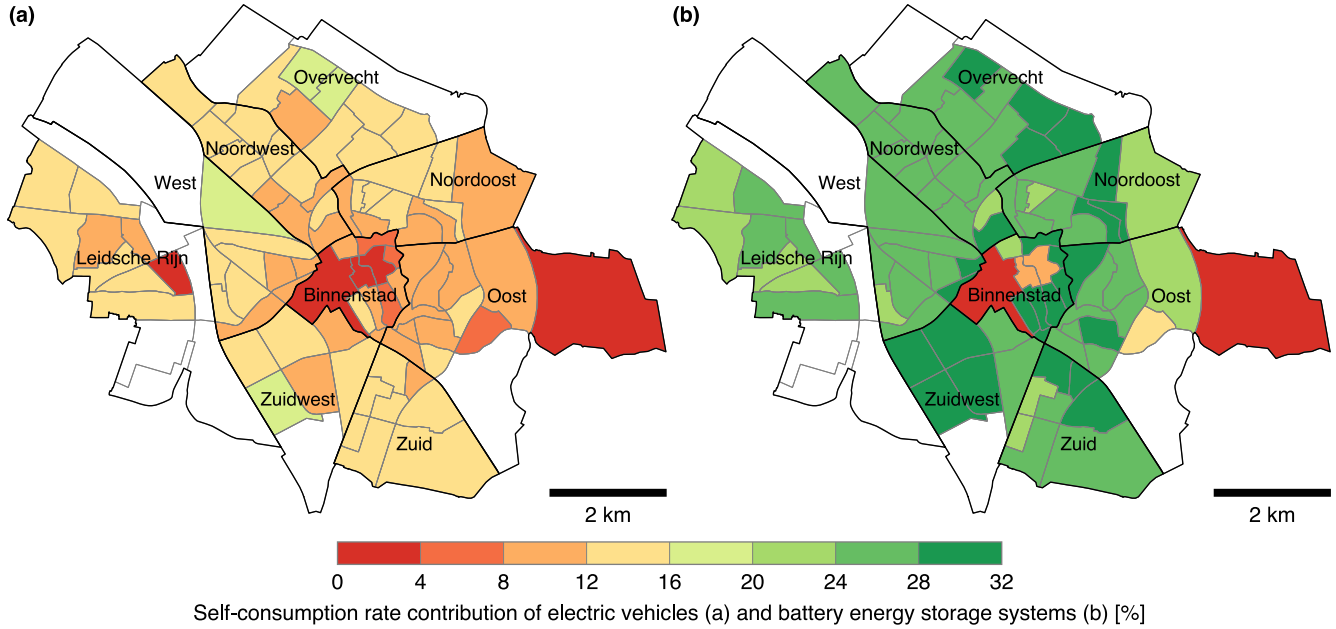

Fig. 7. Potential contribution of electric vehicles to the PV self-consumption ratio (a) and potential contribution of battery energy storage systems to the PV self-consumption ratio (b) for 88 neighbourhoods.

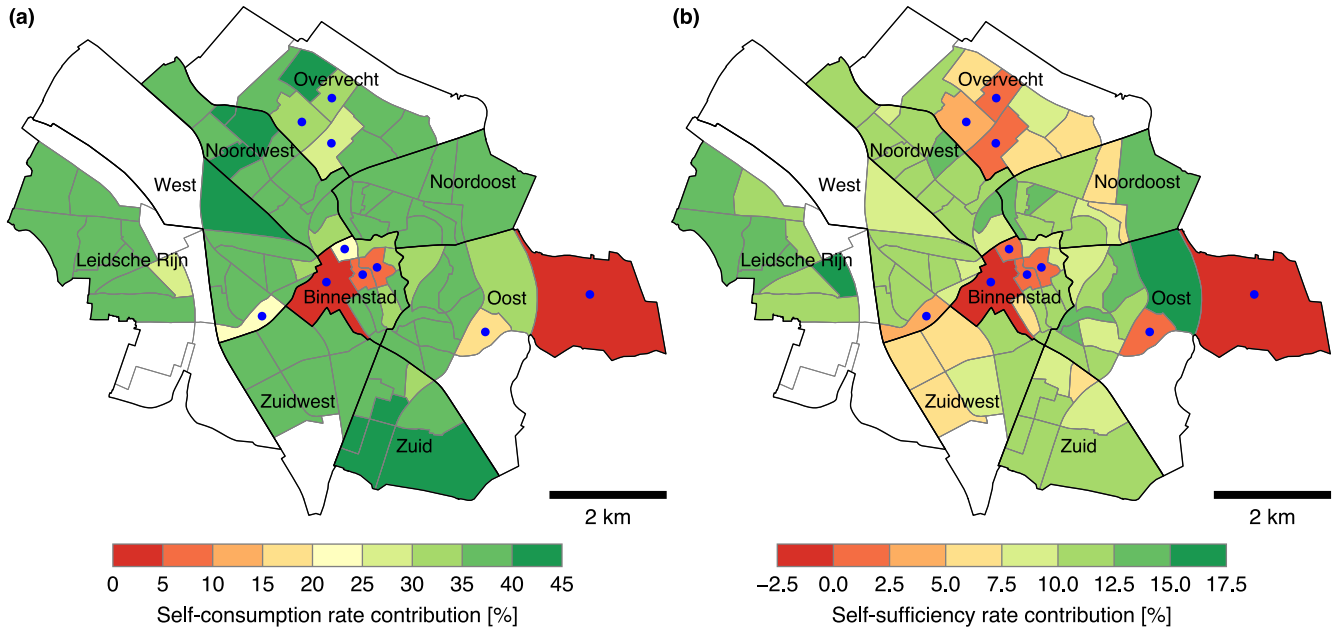

Fig. 8. Potential contribution of electric vehicles with battery energy storage system to the PV self-consumption ratio (a) and contribution to the self-sufficiency ratio (b) for 88 neighbourhoods. Areas with a self-consumption ratio of > 99% are indicated by the blue dot.

result, more electricity is directly used, and less electricity is lost by energy storage conversions. Moreover, some neighbourhoods are surrounded by neighbourhoods with a high initial SCR. For, example the North-West district has a relatively low SCR, but is surrounded by districts with higher SCR. Hence, it could be more beneficial to export surplus PV to these areas, instead of increasing storage capacities. On the other hand the historical inner-city is enclosed by neighbourhoods with lower SCR. These neighbourhoods could provide the inner-city with electricity instead of storing surplus PV electricity in batteries.

3.4. Combined impact of EVs and BESS

The impact of the PV systems with electric vehicles and battery storage on SCR and SSR are presented in Fig. 8. A total of 10 neighbourhoods have a self-consumption ratio of almost 100%, indicated by the blue dots. For the majority of these neighbourhoods a SCR impact of around < 15% is seen. Overall, an average SCR enhancement of 35% can be achieved when EV and storage are added to the neighbourhoods. This results in a high average SCR of 88% within the neighbourhoods, with a range from 67% till 100%.

The self-sufficiency ratios show an average increase of 10% due to EVs and storage, ranging between −0.6% and 16%. The SSR impacts show negative values in two neighbourhoods. These neighbourhoods have a larger additional electricity demand by EVs, than the demand that can be shifted by battery energy storage. Overall, the average SSR increases to 43%, ranging between 6 % and 54%. Also, 17 neighbourhoods have a SSR > 50% with EV and storage.

3.5. Avoided life cycle GHG emissions

The avoided life cycle GHG emissions from an electricity system and neighbourhood perspective were assessed with the reference parameters including electric vehicles and battery energy storage system, see Fig. 9. The avoided GHG emissions are given for the 30-year period per residential address. The emissions show large differences between the neighbourhoods. Avoided GHG emissions from an electricity system perspective are on average 11.5 tCO_2-eq, ranging between 0.3 to 28.1 tCO_2-eq per address. Average avoided GHG emissions from a neighbourhood perspective are 8.6 tCO_2-eq per address, which is around 0.3 tCO_2-eq for each year.

Neighbourhoods with 100% self-consumption ratios have almost similar emissions from an electricity system perspective as from a neighbourhood perspective, since all PV electricity is directly used. These neighbourhoods are located in the centre of the city. The suburb Leidsche Rijn shows high avoided emissions from a neighbourhood perspective, due to high PV potential and the large SCR impact by storage and electric vehicles. The North-West district has similar SCR as the Leidsche Rijn suburb, yet lower avoided emissions are seen here. This is due to the lower electricity demand and the lower PV yield potential for each address in North-West district. The neighbourhood with the lowest self-consumption ratio (Rijnsweerd in the East district) shows the largest emission reductions from system perspective.

PV modules made in Europe are produced with lower greenhouse gas emissions compared to PV made in China, due to the lower carbon intensity of the electricity generation mix in Europe. We compared the impact of PV made in China with PV made in the EU on the avoided emissions. 824 gCO_2-e for each Wp were assumed as emissions from PV produced in Europe (de Wild-Scholten, 2013). The avoided GHG emissions of China and Europe, and the relative change between these areas are shown from an electricity system perspective and neighbourhood perspective in Fig. 10. No change in emissions from manufacturing battery storage was assumed.

When using PV modules manufactured in the EU, the avoided emissions are increasing to averages of 14.4 tCO_2-eq from an electricity perspective and to 11.5 tCO_2-eq from a neighbourhood perspective. The relative change in avoided emissions between China and Europe are significantly higher from a neighbourhood perspective than from an electricity system perspective. An average of 28% is shown for the system perspective and 36% from a neighbourhood perspective. Neighbourhoods with high PV system potential have larger emissions from manufacturing and therefore relatively lower avoided emissions from a neighbourhood perspective. Consequently, the distribution in relative change of avoided emissions from a neighbourhood perspective is larger compared to the avoided emissions from a system perspective.

4. Sensitivity analysis

A sensitivity analysis was conducted for four different rooftop utilization rates. These utilization rates were combined with a larger share of EV solar charging or with smaller or larger battery storage capacities.

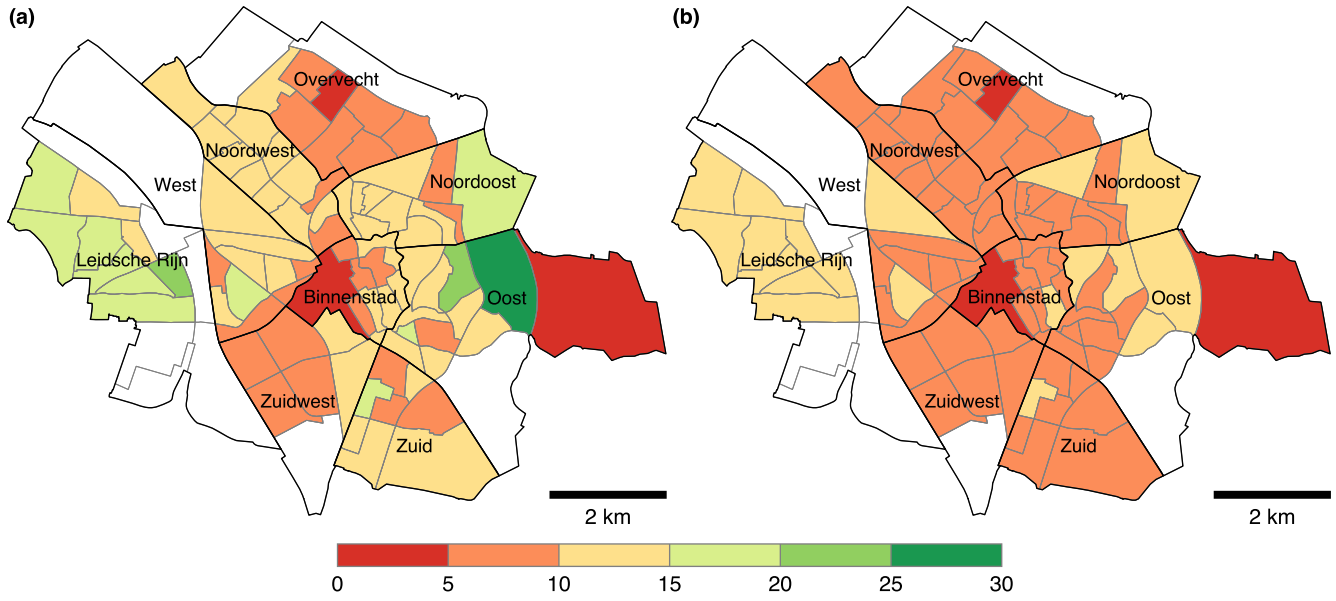

Fig. 9. Potential of avoided life cycle GHG emissions per address from a electricity system perspective (a) and from a neighbourhood perspective (b). The avoided emissions are presented for the reference scenario including electric vehicles and battery storage. Note that the avoided emissions are normalized with the number of addresses within each neighbourhood.

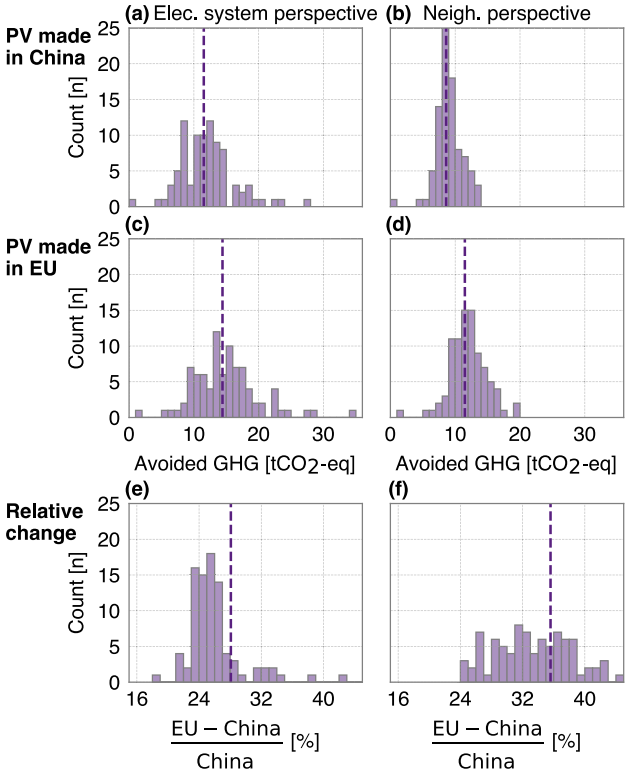

Fig. 10. Distribution of avoided life cycle GHG emissions per address of the neighbourhoods with PV made in China (a & b), PV made in Europe (c & d) and the relative change in avoided emissions between these areas (e & f), The left column shows the avoided emissions from an electricity system perspective and the right columns shows the avoided emissions from a neighbourhood perspective. Mean values of the distribution are indicated by the dashed lines. Histogram bins of 1 tCO_2-eq were used for the avoided emissions and bins of 1% for the relative change. Note that a relative change larger than 45% is observed for one neighbourhoods from a electricity system perspective, and two neighbourhoods from a neighbourhood perspective. These are not shown in histogram (e) and (f).

Other input parameters, see Table 1, were kept constant. Three parameters were assessed; SCR, SSR and avoided life cycle GHG emissions per address from a neighbourhood perspective. The avoided emissions from a system perspective were not shown, since these are less dependent on the PV self-consumption. Some of the scenarios assessed here are not realistic but purely theoretical. A 100% rooftop utilization rate is currently not practical to implement. Moreover, a high smart solar charging share, of 75% or even 100%, requires major investments in charging infrastructures. Furthermore, EVs should be available for charging within the neighbourhood.

4.1. EV smart solar charging share

The influence of five smart solar charging shares of four rooftop utilization rates is presented in Fig. 11. The 25% rooftop utilization scenario shows an average SCR of 85% when no EV is smart charged. This is increased by 11%, if all EVs would apply smart solar charging. In this rooftop utilization scenario, a > 99% SCR is reached for 20 neighbourhoods. This limits the average increase of the SCR. Battery energy storage shows an average SCR close to 100%, for all EV smart charging shares. Thus, energy storage reduces the impact of smart solar charging to almost nothing. Therefore, it is not recommended to invest in smart charging infrastructure with storage under the 25% rooftop utilization rates.

Under the 50% rooftop utilization, a shift from 0% solar charging share to a 100% solar charging share increases the average SCR by 12% points. This is a slightly larger increase than shown for the 25% rooftop utilization rate. Fewer neighbourhoods reach the maximum SCR, thus the average increase in SCR is larger. However, under the 75% rooftop utilization, the increase in SCR due to higher smart charging shares is reduced to 9.6%, which is 2% lower than under the 50% rooftop utilization rate. Higher rooftop utilization rates have significantly more surplus PV available. Therefore, the impact of smart charging share on the SCR is reduced.

Neighbourhoods with storage have a larger PV self-consumption. Consequently, the SCR increase due to a larger solar charging share is reduced to 2.8% points under the 50% rooftop utilization scenario. This number is increased to 3.6% under the 100% rooftop utilization rate, since more surplus PV energy is available for storage. Also, the widest

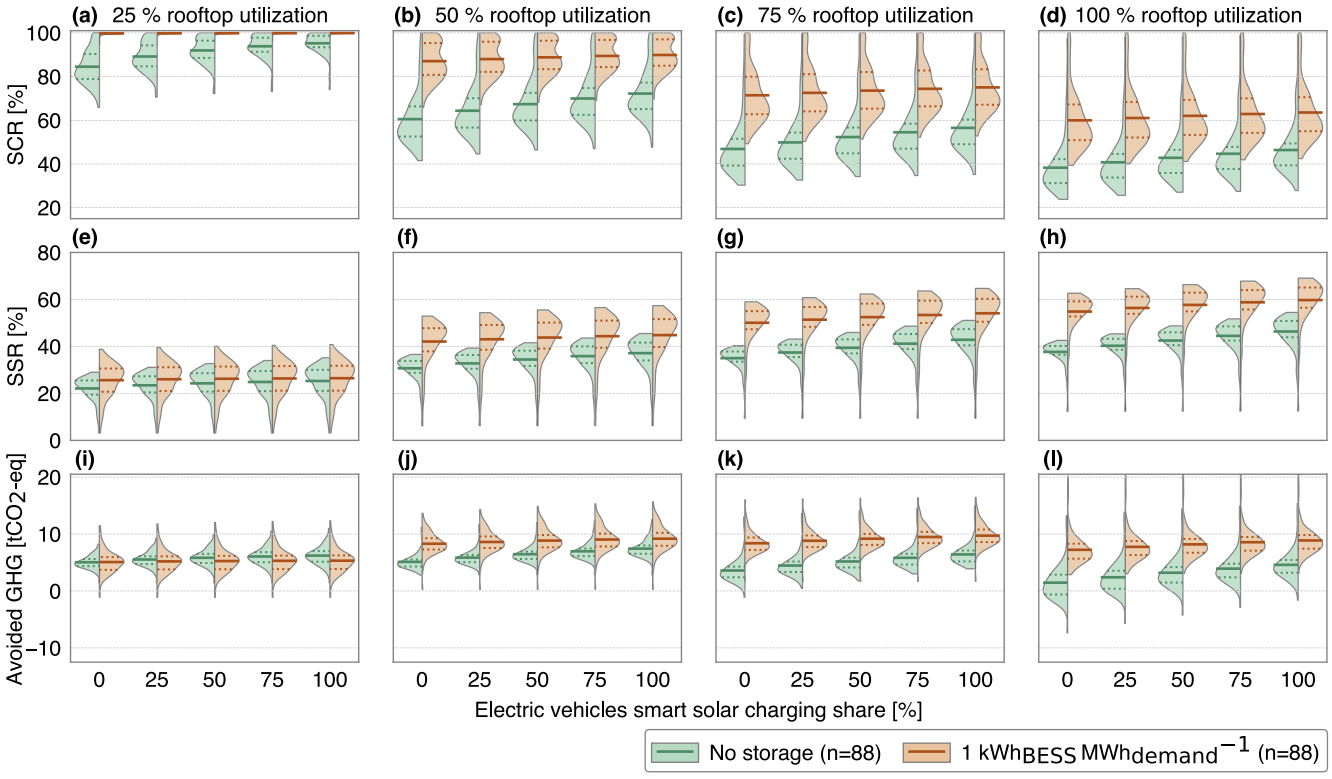

Fig. 11. Influence of the rooftop utilization factor on the self-consumption ratio (a to d), self-sufficiency ratio (e to h) and avoided life cycle emissions per address from a neighbourhood perspective (i to l). The distributions are shown for the 88 neighbourhoods and five electric vehicle charging scenarios using violin plots. The left side of the violin plot shows the distributions without battery storage and the right side of the violin plot shows the distributions with a 1 kWh storage capacity for each MWh of annual electricity consumption. Mean values are indicated by the solid lines and 25% and 75% percentiles are indicated by dotted lines.

distribution between neighbourhoods is seen with a 100% rooftop utilization rate. A larger smart solar charging share reduces the surplus PV that can be stored in batteries. Subsequently, the SCR impact of storage is reduced with higher EV smart solar charging shares. Still, these high smart solar charging shares are not realistic, thus investing in battery energy storage could be worthwhile.

Self-sufficiencies increase slightly for the 25% rooftop utilization rate, with averages from 22% with no smart solar charging to 25% for a 100% solar charging share. SSR are limited when storage is added, with an average of around 26%. Yet, the impact of storage is significantly higher with a 50% utilization rate, and largest for a 100% rooftop utilization rate. Furthermore, the increase in EV smart solar charges share shows a significantly larger impact on the SSR. For a 50% utilization rate and no storage, a shift from 0% to 100% solar charging share results in a SSR increase of 6.5% points. This difference increased by 8.7% points under a 100% rooftop utilization rate. When storage is added to the neighbourhoods, then this increase is 4.8% points. An increase in rooftop utilization rates causes an expansion of the first 25% percentile for both neighbourhoods with and without storage. Neighbourhoods with a low SSR have a far higher electricity demand. Hence, the absolute increase in SSR due to higher PV capacity is smaller for neighbourhoods that already show high SSR.

Avoided life cycle GHG emissions, from a neighbourhood perspective and per addresses, were found to be increasing from a 25% to a 75% rooftop utilization rate. However, the avoided emissions have decreased for a 100% rooftop utilization compared to a 75% rooftop utilization. Some neighbourhoods even showed negative values. This means that the emissions due to manufacturing of PV and storage systems are larger than the avoided emissions due to the direct consumption at the neighbourhood level. Furthermore, under the 25% rooftop utilization rate, avoided emissions are lower for neighbourhoods with storage than without storage.

Yet, from an electricity system perspective, the average avoided emissions increased by rooftop utilization rates. Neighbourhoods without storage and a 25% solar smart share showed averages of 7, 14, 21 and 27 tCO_2-eq of avoided emissions for 25, 50, 75 and 100% rooftop utilization rates respectively. Neighbourhoods with storage and a 25% solar smart share showed lower avoided emissions of 5, 12, 18 and 25 tCO_2-eq of for 25, 50, 75 and 100% rooftop utilization rates respectively.

4.2. Battery storage capacity

The influence of increasing battery storage capacities under four rooftop utilization rates is presented in Fig. 12. SCR increased under all scenarios with larger storage capacities and when EVs are included. With 25% of rooftop utilization, the SCR is maximized with the use of energy storage and electric vehicles. With 50% rooftop utilization, we found that a 2 kWh storage system per MWh demand does not impact the upper 25% percentile of the neighbourhoods. Hence, a quarter of the neighbourhoods can consume all locally produced PV electricity under these conditions. A 75% and 100% rooftop utilization rate results in a higher impact of larger battery storage capacities. The addition of electric vehicles to the neighbourhoods results in higher SCR values. For these high rooftop utilization rates, the average SCR impact from energy storage is quite similar for neighbourhoods with and without EVs. Also in this case, surplus PV electricity is not fully utilized by EVs charging and therefore storage can have a similar impact. Furthermore, additional demand is added with EVs, which results in relatively larger storage capacities and thus higher SCR.

Self-sufficiency ratios gradually increase with higher rooftop utilization rates. With 25% rooftop utilization, the highest SSR were observed for a battery size of 1 kWh per MWh demand. Larger storage capacities resulted in more electricity losses caused by charging and

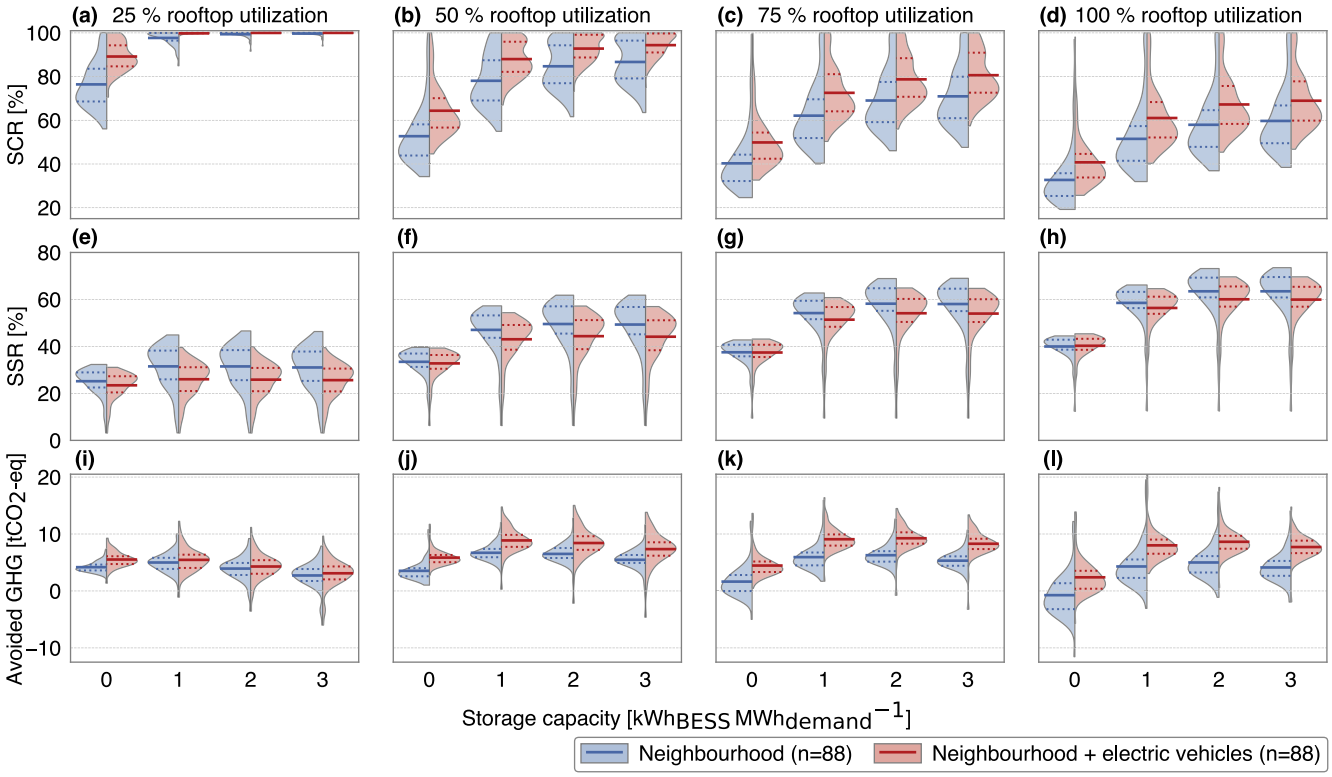

Fig. 12. Influence of the rooftop utilization factor on the self-consumption ratio (a to d), self-sufficiency ratio (e to h) and avoided life cycle emissions per address from a neighbourhood perspective (i to l). The distributions are shown for the 88 neighbourhoods and four battery storage capacities using violin plots. The left side of the violin plot shows the distributions with electricity consumption of the neighbourhood only and the right side of the violin plot shows the distributions of the neighbourhood with electric vehicles. The electric vehicles have a 25% solar charging share. Mean values are indicated by the solid lines and 25% and 75% percentiles are indicated by dotted lines.

discharging of the batteries. Consequently, self-sufficiency is reduced within the neighbourhood.

Neighbourhoods with EVs have a higher direct PV self-consumption, thus less surplus PV electricity can be shifted by storage. As a result, the influence of storage is smaller for neighbourhoods with EVs than for neighbourhoods without EVs. Under the no storage scenarios, almost similar SSR distributions were observed for neighbourhoods with EVs and without EVs. This indicates that power consumption time series of the EVs is comparable to the electricity consumption time series of the neighbourhoods.

Avoided emissions per address are largely dependent on rooftop utilization rate and installed storage capacities. Under the 25% rooftop utilization scenario, the increase in storage capacity shows a significant reduction in avoided emissions. For higher rooftop utilization rates, an increase in avoided emissions can be seen when shifting from no storage to 1 kWh per MWh capacity. However, larger storage capacities show a reduction of avoided emissions. For these larger capacities, the emissions due to manufacturing are higher than the avoided emissions due to the self-consumption. Moreover, EVs add demand to the neighbourhood and therefore avoided life-cycle emissions increase.

5. Discussion

This research showed that PV self-consumption and self-sufficiency potential varies significantly between neighbourhoods. These variations are primarily related to limited residential roof area for PV siting, higher electricity demand, or higher expected electric vehicle penetration rates. A number of limitations concerning assumptions and data availability were made in this research that could impact the outcome substantially.

5.1. Data limitations

The PV potential of facades from residential buildings was not included in the study. Especially, facades from tall residential buildings can significantly increase the PV potential in neighbourhoods (Freitas et al., 2018). For example, the district of Overvecht contains numerous tall residential buildings, consequently limiting the self-sufficiency ratio. Also, including facades would substantially increase the self-sufficiency ratio of these types of buildings. Furthermore, by using east and west oriented facades, the PV yield over the day is extended beyond the noon peak to early morning and late afternoon. This will provide a higher direct PV self-consumption and decrease the need for storage (Litjens et al., 2017). However, assessment of PV potential of facades is computation-intensive, since another dimension is added to the radiation model (Catita et al., 2014). Furthermore, information about the share of windows and other building facade components makes the model complex. In addition, this information is not easily available.

The annual incoming POA irradiance on each rooftop was assessed using the ARCGIS tools. This number was used to linearly scale down PV yield time series obtained from the PVLIB model. Consequently, we assumed that the shade was homogenous homogeneously spread over the PV yield time series. However, the impact of shade on the PV yield depends on the position of the sun in the sky and the location of the obstructions which block the direct sunlight. We aggregated the individual PV time series of each roof to a time series for a neighbourhood. Also, we assumed the shades on each PV system in the neighbourhood do not occur simultaneously. Subsequently, the influence ofshade on individual PV system decreases. Determining incoming POA irradiance for each roof for a smaller time step is recommended for further research. However, this requires significant more computation time or different calculation tools. Furthermore, we assumed that all incoming irradiance on the PV module would be converted to

electricity. This conversion could be decreased due to partial shading of the module. The impact of partial shading on the PV yield depends on the installed system architecture and the module design (Sinapis et al., 2016).

We used one year of data (2015) to assess the rooftop PV potential and corresponding PV integration parameters, due to data availability and computation time. The year 2015 had a relative high annual irradiance compared to pre 2015 years (Litjens et al., 2017). Consequently, the PV yield production is overestimated with a few percent. Subsequently a higher self-consumption is expected but also a lower self-sufficiency. Furthermore, we assumed that excess PV power is distributed to other residential buildings within the neighbourhood using the low voltage grid. Power and voltage constraints within the low voltage grid were not considered. A detailed map of the low voltage grid should be included for future research for assessment of these potential limitations.

We assumed a constant emission factor for electricity over the year. Consequently, results showed that storage does not contribute to emission reductions from an electricity system perspective. However, with a larger share of renewables, a higher variability of emission factors from power generation can be expected. Consequently, the avoided emissions from storage could increase. If batteries would discharge at moments with a large share of fossil fuel fired power plants in the power generation mix, then this would avoid more emissions. Battery control strategies that include the marginal emissions factor should be developed.

5.2. Implementation considerations

Currently, over 90% of residential buildings are heated using natural gas-based systems (Joost Gerdes and Sjoerd Marbus and Martijn Boelhouwer, 2016). The Dutch government has set goals to replace these with other technologies, e.g. heat pumps. This could increase the electricity demand of cities in the Netherlands. But the expected electricity demand of heat pumps in cities is hard to predict. Firstly, the residential buildings should be selected in which heat pumps are the most economically viable option to replace natural gas boilers. For example, district heating systems can also be used to replace natural gas heating systems, especially in densely populated cities (Lake et al., 2017). Secondly, the electricity demand of heat pumps mainly depends on the heat source (air or ground) and the characteristics of the buildings. Especially old buildings should be insulated before installation of any heat pump system. The assessment of future electricity demand from residential buildings due to electric heating is highly recommended in future research.

The electricity demand for electric vehicles could be underestimated if more people will charge their EV within the city than was assumed. This could potentially occur when fast charging stations are introduced within the city, yet this would also require additional grid expansion measures. On the other hand, this demand could be overestimated due to reduced policy support for charging stations within cities. Furthermore, car sharing could result in less need for privately owned cars, and therefore reduce the demand. Moreover, a lack of parking spots or improved public transport can reduce the number of electric vehicles.

The technical PV potential in our study was assessed using 50% of the roof area. However, the estimated economic potential is lower due to the following reasons. First, the net-metering policy is established in the Netherlands. Consequently, dwelling owners with a relative large roof area will probably only install a PV capacity sufficient to provide in their annual electricity consumption. Second, PV systems with a relative low specific PV yield will not be installed due to a significantly larger payback period.

PV power density of 200 Wp/m^2 are assumed, but are expected to increase in the future due to higher module efficiencies. This would increase the PV yield potential and decrease the self-consumption, but increase the self-sufficiency. Also, we expect that future cost of PV systems will decrease based on the historical learning rates of around 20% (Louwen et al., 2016). Consequently, the economic profitability of PV systems for orientations with lower incoming irradiance will increase.

6. Conclusion

This study developed a spatio-temporal model that aimed to assess residential PV electricity integration options. The impact of electricity consumptions from buildings, electric vehicles and battery energy storage system was investigated for each neighbourhood in the city of Utrecht, the Netherlands. A large variety in PV yield potential, self-consumption ratio and self-sufficiency ratio was found between the neighbourhoods. Self-consumption ratios are between 34% and 100% for the neighbourhoods. This could be increased on average by 12% by electric vehicles and 25% with battery storage. Avoided life cycle emissions are between 0 and 28 tCO_2-eq, with an average of 12 tCO_2-eq per address.

The spatial analysis identified neighbourhoods with potential surplus PV electricity that could be used to provide electricity to surrounding neighbourhoods with lower PV potential. We recommend using battery storage capacities only in areas in which storage has a high impact on self-consumption enhancement. Also, supporting policies for smart solar charging of electric vehicles should focus on neighbourhoods with large PV potential and relatively low electricity consumption. Especially for neighbourhoods were the low voltage grids require considerable expansion to host the potential PV capacity. Moreover, PV supporting policies should focus on neighbourhoods with a higher potential of avoided life cycle GHG emissions. The dissimilarity of results between the neighbourhoods indicates that area dependent investments and supporting policies could improve the PV power integration in cities. Therefore, we recommend the use of our spatio-temporal model for other cities to assist local governments and district system operators in the transition towards sustainable cities.

Acknowledgment

This work is funded by three projects. First, the research programme Transitioning to a More Sustainable Energy System (Grant No. 022.004.023), funded by the Netherlands Organisation for Scientific Research (NWO). Second, the Advanced Solar Monitoring project, funded by the Netherlands Enterprise Agency RVO (Grant No. TKIZ01015). Third, the Advanced Scenario Management - Phase 2, funded by the Netherlands Enterprise Agency RVO (Grant No. TEUE116903). We are grateful to the Royal Netherlands Meteorological Institute for providing data.

References

Actueel Hoogte Bestand Nederland. Wijk- en buurtkaart 2016, 2016. <http://www.ahn.nl/index.html>.

Acuto, M., 2016. Give cities a seat at the top table. Nature 537 (7622), 611–613. https://doi.org/10.1038/537611a.

Ajanovic, A., Haas, R., 2015. Driving with the sun: why environmentally benign electric vehicles must plug in at renewables. Sol. Energy 121, 169–180. https://doi.org/10.1016/j.solener.2015.07.041.

Andrews, R.W., Stein, J.S., Hansen, C., Riley, D., 2014. Introduction to the open source PV LIB for python photovoltaic system modelling package. In: 2014 IEEE 40th Photovoltaic Specialist Conference (PVSC). IEEE. https://doi.org/10.1109/pvsc.2014.6925501.

Assouline, D., Mohajeri, N., Scartezzini, J.-L., 2018. Large-scale rooftop solar photovoltaic technical potential estimation using random forests. Appl. Energy 217, 189–211. https://doi.org/10.1016/j.apenergy.2018.02.118.

Bottaccioli, L., Estebsari, A., Patti, E., Pons, E., Acquaviva, A., 2017. A novel integrated real-time simulation platform for assessing photovoltaic penetration impacts in smart grids. Energy Proc. 111, 780–789. https://doi.org/10.1016/j.egypro.2017.03.240.

Camargo, L.R., Zink, R., Dorner, W., Stoeglehner, G., 2015. Spatio-temporal modeling of roof-top photovoltaic panels for improved technical potential assessment and electricity peak load offsetting at the municipal scale. Comput., Environ. Urban Syst. 52,

58–69. https://doi.org/10.1016/j.compenvurbsys.2015.03.002.
Catita, C., Redweik, P., Pereira, J., Brito, M., 2014. Extending solar potential analysis in buildings to vertical facades. Comput. Geosci. 66, 1–12. https://doi.org/10.1016/j.cageo.2014.01.002.
Centraal Bureau voor de Statistiek. Verkeersprestaties personenauto's, leeftijd uitgebreid, brandstof, 2016a. <http://statline.cbs.nl/StatWeb/publication/?VW=T&DM=&PA=83702NED&D1=a&D2=0&D3=a&D4=a&HD=171009-0949&HDR=T,G3&STB=G1,G2>.
Centraal Bureau voor de Statistiek. Wijk- en buurtkaart 2016, 2016b. <https://www.cbs.nl/nl-nl/dossier/nederland-regionaal/geografische%20data/wijk-en-buurtkaart-2016>.
Centraal Bureau voor de Statistiek. Rendementen en CO2-emissie elektriciteitsproductie 2016, 2018. <https://www.cbs.nl/nl-nl/maatwerk/2018/04/rendementen-en-co2-emissie-elektriciteitsproductie-2016>.
de Wild-Scholten, M.M., 2013. Energy payback time and carbon footprint of commercial photovoltaic systems. Sol. Energy Mater. Sol. Cells 119, 296–305. https://doi.org/10.1016/j.solmat.2013.08.037.
Defaix, P., van Sark, W., Worrell, E., de Visser, E., 2012. Technical potential for photovoltaics on buildings in the EU-27. Sol. Energy 86 (9), 2644–2653. https://doi.org/10.1016/j.solener.2012.06.007.
Enphase Energy. Enphase M215, 2015. <https://www.enphase.com/sites/default/files/M215_DS_EN_60Hz.pdf>.
Environmental Systems Research Institute (Esri). ArcGIS Spatial Analyst, 2017. <http://www.esri.com/software/arcgis/extensions/spatialanalyst>.
European Commission. Best practices on Renewable Energy Self-consumption Accompanying. Technical report, European Commission, Brussels, 2015.
Freitas, S., Catita, C., Redweik, P., Brito, M., 2015. Modelling solar potential in the urban environment: state-of-the-art review. Renew. Sustain. Energy Rev. 41, 915–931. https://doi.org/10.1016/j.rser.2014.08.060.
Freitas, S., Reinhart, C., Brito, M., 2018. Minimizing storage needs for large scale photovoltaics in the urban environment. Sol. Energy 159, 375–389. https://doi.org/10.1016/j.solener.2017.11.011.
Fu, P., Rich, P.M., 2002. A geometric solar radiation model with applications in agriculture and forestry. Comput. Electron. Agric. 37 (1–3), 25–35. https://doi.org/10.1016/s0168-1699(02)00115-1.
Hawkins, T.R., Singh, B., Majeau-Bettez, G., Strømman, A.H., 2012. Comparative environmental life cycle assessment of conventional and electric vehicles. J. Indus. Ecol. 17 (1), : 53–64. https://doi.org/10.1111/j.1530-9290.2012.00532.x.
Het kadaster. Basisregistraties Adressen en Gebouwen (BAG), 2016. <https://www.kadaster.nl/bag>.
Hofierka, J., Kaňuk, J., 2009. Assessment of photovoltaic potential in urban areas using open-source solar radiation tools. Renew. Energy 34 (10), 2206–2214. https://doi.org/10.1016/j.renene.2009.02.021.
Hoogvliet, T., Litjens, G., van Sark, W., 2017. Provision of regulating- and reserve power by electric vehicle owners in the Dutch market. Appl. Energy 190, 1008–1019. https://doi.org/10.1016/j.apenergy.2017.01.006.
Hoppmann, J., Volland, J., Schmidt, T.S., Hoffmann, V.H., 2014. The economic viability of battery storage for residential solar photovoltaic systems – a review and a simulation model. Renew. Sustain. Energy Rev. 39, 1101–1118. https://doi.org/10.1016/j.rser.2014.07.068.
Joost Gerdes and Sjoerd Marbus and Martijn Boelhouwer. Energietrends 2016. Technical report, September 2016.
Jordan, D.C., Kurtz, S.R., VanSant, K., Newmiller, J., 2016. Compendium of photovoltaic degradation rates. Prog. Photovolt.: Res. Appl. 24 (7), 978–989. https://doi.org/10.1002/pip.2744.
Kausika, B.B., Dolla, O., Folkerts, W., Siebenga, B., Hermans, P., van Sark, W.G.J.H.M., 2015. Bottom-up Analysis of the Solar Photovoltaic Potential for a City in the Netherlands - A Working Model for Calculating the Potential using High Resolution LiDAR Data. In: Proceedings of the 4th International Conference on Smart Cities and Green ICT Systems. SCITEPRESS - Science and Technology Publications. https://doi.org/10.5220/0005431401290135.
Kausika, B., Moraitis, P., van Sark, W., 2018. Visualization of operational performance of grid-connected PV systems in selected european countries. Energies 11 (6), 1330. https://doi.org/10.3390/en11061330.
Lake, A., Rezaie, B., Beyerlein, S., 2017. Review of district heating and cooling systems for a sustainable future. Renew. Sustain. Energy Rev. 67, 417–425. https://doi.org/10.1016/j.rser.2016.09.061.
Liander N.V.. Liander Open data, 2016. <https://www.liander.nl/over-liander/innovatie/open-data/data>.
Litjens, G., Worrell, E., van Sark, W., 2017. Influence of demand patterns on the optimal orientation of photovoltaic systems. Sol. Energy 155, 1002–1014. https://doi.org/10.1016/j.solener.2017.07.006.
Litjens, G., Worrell, E., van Sark, W., 2018a. Assessment of forecasting methods on performance of photovoltaic-battery systems. Appl. Energy 221, 358–373. https://doi.org/10.1016/j.apenergy.2018.03.154.
Litjens, G., Worrell, E., van Sark, W., 2018b. Economic benefits of combining self-consumption enhancement with frequency restoration reserves provision by photovoltaic-battery systems. Appl. Energy 223, 172–187. https://doi.org/10.1016/j.apenergy.2018.04.018.
Louwen, A., van Sark, W.G.J.H.M., Faaij, A.P.C., Schropp, R.E.I., 2016. Re-assessment of net energy production and greenhouse gas emissions avoidance after 40 years of photovoltaics development. Nat. Commun. 7, 13728. https://doi.org/10.1038/ncomms13728.
Luthander, R., Widén, J., Nilsson, D., Palm, J., 2015. Photovoltaic self-consumption in buildings: a review. Appl. Energy 142, 80–94. https://doi.org/10.1016/j.apenergy.2014.12.028.
Mainzer, K., Fath, K., McKenna, R., Stengel, J., Fichtner, W., Schultmann, F., 2014. A high-resolution determination of the technical potential for residential-roof-mounted photovoltaic systems in Germany. Sol. Energy 105, 715–731. https://doi.org/10.1016/j.solener.2014.04.015.
Masson, G., Kaizuka, I., 2017. Trends 2017 in photovoltaic applications. Technical report, International Energy Agency; Photovoltaic Power Systems Programme.
Molin, A., Schneider, S., Rohdin, P., Moshfegh, B., 2016. Assessing a regional building applied PV potential – spatial and dynamic analysis of supply and load matching. Renew. Energy 91, 261–274. https://doi.org/10.1016/j.renene.2016.01.084.
Mu, Y., Wu, J., Jenkins, N., Jia, H., Wang, C., 2014. A spatial–temporal model for grid impact analysis of plug-in electric vehicles. Appl. Energy 114, 456–465. https://doi.org/10.1016/j.apenergy.2013.10.006.
Munkhammar, J., Bishop, J.D., Sarralde, J.J., Tian, W., Choudhary, R., 2015. Household electricity use, electric vehicle home-charging and distributed photovoltaic power production in the city of westminster. Energy Build. 86, 439–448. https://doi.org/10.1016/j.enbuild.2014.10.006.
Mwasilu, F., Justo, J.J., Kim, E.-K., Do, T.D., Jung, J.-W., 2014. Electric vehicles and smart grid interaction: a review on vehicle to grid and renewable energy sources integration. Renew. Sustain. Energy Rev. 34, 501–516. https://doi.org/10.1016/j.rser.2014.03.031.
Nykvist, B., Nilsson, M., 2015. Rapidly falling costs of battery packs for electric vehicles. Nat. Climate Change 5 (4), 329–332. https://doi.org/10.1038/nclimate2564.
Panasonic. Panasonic HIP-225HDE1, 2015. <http://www.technosun.com/eu/products/solar-module-SANYO-HIP-225HDE1.php>.
Peters, J.F., Baumann, M., Zimmermann, B., Braun, J., Weil, M., 2017. The environmental impact of li-ion batteries and the role of key parameters – a review. Renew. Sustain. Energy Rev. 67, 491–506. https://doi.org/10.1016/j.rser.2016.08.039.
Rich, P., R., D., W.A., H., S.C., S., 1994. Using viewshed models to calculate intercepted solar radiation: Applications in ecology. American Society for Photogrammetry and Remote Sensing Technical Papers, 66, pp. 524–529.
Rodríguez, L.R., Duminil, E., Ramos, J.S., Eicker, U., 2017. Assessment of the photovoltaic potential at urban level based on 3d city models: a case study and new methodological approach. Sol. Energy 146, 264–275. https://doi.org/10.1016/j.solener.2017.02.043.
Schmidt, O., Hawkes, A., Gambhir, A., Staffell, I., 2017. The future cost of electrical energy storage based on experience rates. Nat. Energy 2 (8), 17110. https://doi.org/10.1038/nenergy.2017.110.
Schram, W.L., Lampropoulos, I., van Sark, W.G., 2018. Photovoltaic systems coupled with batteries that are optimally sized for household self-consumption: assessment of peak shaving potential. Appl. Energy 223, 69–81. https://doi.org/10.1016/j.apenergy.2018.04.023.
Sijm, J., Gockel, P., de Joode, J., van Westering, W., Musterd, M., 2017. The demand for flexibility of the power system in the netherlands, 2015-2050, report of phase 1 of the flexnet project. Technical report, ECN & Alliander, November 2017.
Sinapis, K., Tzikas, C., Litjens, G., van den Donker, M., Folkerts, W., van Sark, W., Smets, A., 2016. A comprehensive study on partial shading response of c-Si modules and yield modeling of string inverter and module level power electronics. Sol. Energy 135, 731–741. https://doi.org/10.1016/j.solener.2016.06.050.
SMA Solar Technology AG. Sunny Boy Storage 2.5, 2017. <https://www.sma.de/en/products/battery-inverters/sunny-boy-storage-25.html#Downloads-236248>.
Sociaal-Economische Raad. The Agreement on Energy for Sustainable Growth. Technical report, Sociaal-Economische Raad (Social and Economic Council), 2015. <https://www.energieakkoordser.nl/~/media/files/energieakkoord/publiciteit/agreement-on-energy-policy-in-practice.ashx>.
Stedin Holding N.V. Stedin Verbruiksgegevens, 2016. <https://www.stedin.net/zakelijk/open-data/verbruiksgegevens>.
Tesla Motors, Inc. Tesla Motors, Inc. Powerwall Product Homepage, 2016. <http://www.teslamotors.com/nl_NL/powerwall>.
Truong, C., Naumann, M., Karl, R., Müller, M., Jossen, A., Hesse, H., 2016. Economics of residential photovoltaic battery systems in Germany: The Case of Tesla's Powerwall. Batteries 2 (4), 14. https://doi.org/10.3390/batteries2020014.
van der Kam, M., van Sark, W., 2015. Smart charging of electric vehicles with photovoltaic power and vehicle-to-grid technology in a microgrid; a case study. Appl. Energy 152, 20–30. https://doi.org/10.1016/j.apenergy.2015.04.092.
van der Kam, M., Meelen, A., van Sark, W., Alkemade, F., 2018. Diffusion of solar photovoltaic systems and electric vehicles among dutch consumers: implications for the energy transition. Energy Res. Soc. Sci. 46, 68–85. https://doi.org/10.1016/j.erss.2018.06.003.
Wegertseder, P., Lund, P., Mikkola, J., Alvarado, R.G., 2016. Combining solar resource mapping and energy system integration methods for realistic valuation of urban solar energy potential. Sol. Energy 135, 325–336. https://doi.org/10.1016/j.solener.2016.05.061.
Yamagata, Y., Seya, H., 2013. Community-based resilient electricity sharing: optimal spatial clustering. In: 2013 43rd Annual IEEE/IFIP Conference on Dependable Systems and Networks Workshop (DSN-W). IEEE. https://doi.org/10.1109/dsnw.2013.6615539.